Active and Passive Elec. Comp., 2000, Vol. 23, pp. 37–51
Reprints available directly from the publisher
Photocopying permitted by license only

CHEMICAL ETCHING OF {hk0} SILICON PLATES IN EDP PART I: EXPERIMENTS AND COMPARISON WITH TMAH

C. R. TELLIER*, T. G. LEBLOIS and A. CHARBONNIERAS

Laboratoire de Chronométrie, Electronique et Piézoélectricité, Ecole Nationale Supérieure de Mécanique et des Microtechniques, 26 Chemin de l'Epitaphe, 25030 Besancon Cedex, France

(Received 12 April 2000; In final form 25 April 2000)

This paper deals with the anisotropic chemical etching of various silicon plates etched in EDP. Changes with orientation in geometrical features of etched surface and in the etching shape of starting circular sections are systematically investigated. These etching shapes are compared with shapes produced by etching in KOH and TMAH solutions; This experimental study allows us to determine the dissolution slowness surface for the EDP solution and to investigate the real influence of the etchant on two dimensional and three dimensional etching shapes.

Keywords: Etching; Silicon plates; EDP solution

1. INTRODUCTION

In the last decade there is a continuous development of the chemical etching of silicon crystal. Emphasis is placed on etchants used for the bulk micromachining of silicon micromechanical devices [1–7] such as EDP [1, 5] and KOH [1–3] solutions or such TMAH based etchants [6, 7] whose interest in micromachining is still in evaluation actually. Most of works [1, 4–6] were devoted to {100} or {110} surfaces even if for mechanical sensors applications other orientations such as {hhl} planes are of interest [8]. This paper replies to this need and an extensive study of the geometrical features of {hk0} silicon surfaces

*Corresponding author. e-mail: ctellier@ens2m.fr

etched in an EDP solution is undertaken. In addition modifications in the shape of starting circulate plates are also investigated. Finally attempts are made to compare the behaviour for the three etchants from a practical point of view with a special attention to EDP and TMAH etchants which are known to be compatible with IC fabrication processes [1, 6, 7].

2. EXPERIMENTALS

2.1. Experimental Details

Twelve differently-oriented silicon circular plates (1,5 mm thick) corresponding to the $(h\bar{k}0)$ planes listed in Table I were cut in a silicon ingot. The two surfaces and the side contour of plates were mechanically lapped and then optically polished. The etching experiments for the EDP etchant (ED: 75 ml, P: 24 g, H_2O: 24 ml) were carried out with an etching bath maintened at a constant temperature of $118 \pm 0.5°C$ for successive periods of time. A glass refluxing system was used to prevent composition change by loss of volatile matter.

Moreover various {hk0} plates suffer successive isothermal etchings at $80 \pm 0.5°C$ in the two other etchants (35% KOH-water and 25% TMAH-water). After each isothermal etching the etch rates were determined by using a "Palmer" instrument which provides an accuracy of about 1 μm.

The changes in starting circular cross-sections were investigated by using a Talyrond analyser which generates magnified out-of-roundness profiles with the superimposed least mean square circle.

The surface texture of etched silicon plates were examined by scanning electron microscopy (SEM) and by atomic force microscopy (AFM). The image software of the AFM includes surface profile plots along selected lines. In addition surface profilometry traces were made using a mechanical profilometer coupled with a computer.

TABLE I Values for the angles of cut, φ_o, and identification of Miller indices for the corresponding (hkl) plane in the vicinity of the reference surface. Only Miller indices smaller than 10 are indicated

φ_o(*deg.*)	0	5	10	14	18	23	26	30	34	37	42	45
hkl	010	–	$\bar{6}10$	$\bar{4}10$	$\bar{3}10$	$\bar{7}30$	$\bar{2}10$	$\bar{7}40$	$\bar{3}20$	$\bar{4}30$	$\bar{9}80$	$\bar{1}10$

2.2. The Etch Rate

For the (h$\bar{k}$0) plates the dissolution rate R (h$\bar{k}$0) is identified as the ratio of the decrement Δd in the thickness d over the duration of isothermal etching t. Variations in the total decrement in thickness as a function of the angle of cut φ_o are shown in Figure 1 for three successive isothermal etchings. We observe that the etch rate is affected by the total duration of etching and that in fact R is smaller at the beginning of the etching process than after the second and third isothermal etchings. This behaviour can be partly explained by the progressive degradation of etched surfaces as discussed in Section 2.3.

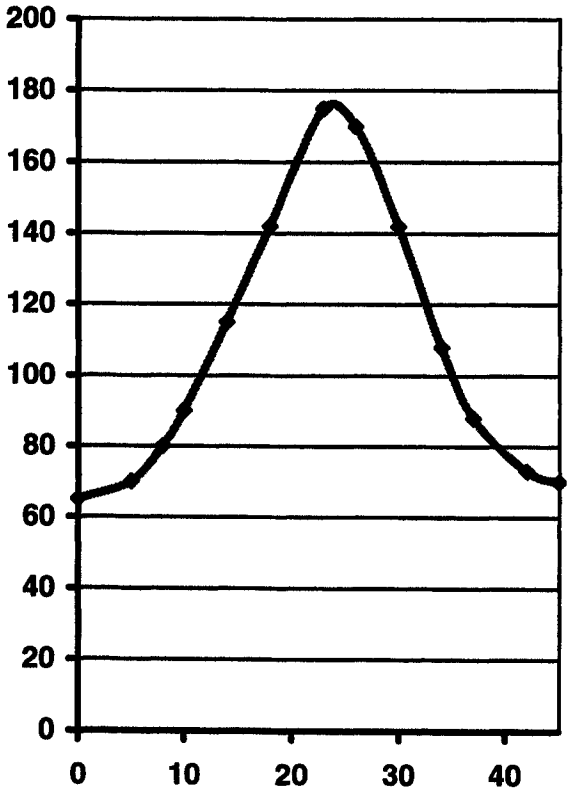

FIGURE 1 Evolution in the total decrement in thickness d (in μm) with the angle of cut φ_o for three successive isothermal etchings of $\Delta t = 15$ min.

2.3. Geometrical Features of Etched Surfaces

S.E.M. observations (Figs. 2 and 3) of the various (hk̄0) surfaces reveal that, for a given cut, the two surfaces are entirely covered by dissolution figures fitted into each other whose geometrical features are characteristic of the angle of cut φ_o. In particular as the angle of cut increases from 0° to 45° we observe (Fig. 2) the formation of flat hillocks ((100) plane, Fig. 2a), of somewhat convex pits (in the vicinity of (120) plane, Figs. 2d and 2e) or of very flat grooves ((110) plane, Fig. 3). These characteristic dissolution figures develop in the first stage of etching and prolonged etchings induce an increase in the lateral size of dissolution figures (Fig. 3). For convenience Table II summarizes briefly the main features of dissolution figures as viewed on the SEM images of Figures 2 and 3. Moreover it is also of interest to study the influence of the total duration of etching t on the

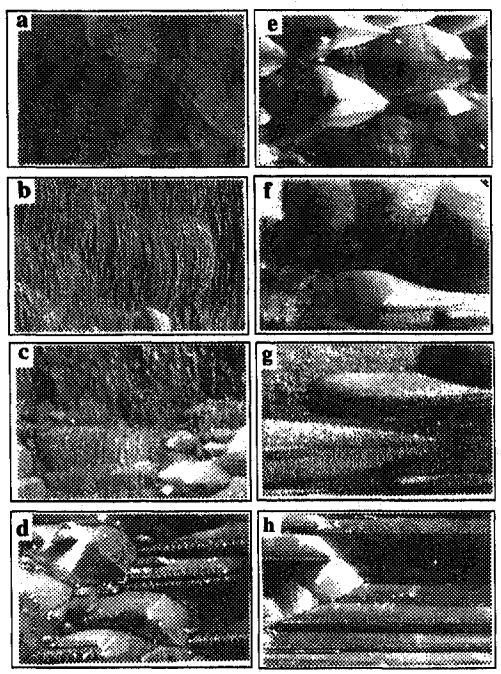

FIGURE 2 SEM images of some (hk̄0) plates after etching in EDP. Cases of $\varphi_o = 0°$ (a), $\varphi_o = 10°$ (b), $\varphi_o = 14°$ (c), $\varphi_o = 23°$ (d), $\varphi_o = 26°$ (e), $\varphi_o = 34°$ (f), $\varphi_o = 37°$ (g), $\varphi_o = 42°$ (h).

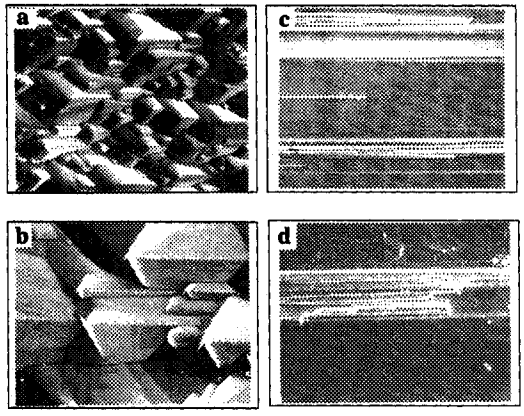

FIGURE 3 SEM images of some (hk̄0) plates after 15 min etching ((a) for $\varphi_o = 30°$, (c) for $\varphi_o = 45°$), and after 45 min etching ((b) for $\varphi_o = 30°$, (d) for $\varphi_o = 45°$).

TABLE II Geomentrical features of final dissolution figures as revealed by SEM examination of Figure 2

Angle of cut φ_o (°)	*General features*
0°	Flat pits
10°	Bumpy dissolution figures aligned along the rotated axis X'
14°	Features close to those related to $\varphi_o = 10°$
18°	Features close to those related to $\varphi_o = 14°$
26°	Bumpy hillocks partly bounded by "limiting facets " and aligned along X' axis
30°	Hillocks aligned along X' and composed of "limiting facets"
37°	Elongated hillocks composed of limiting facets
42°	Grooves aligned along the X' axis
45°	Flat concave grooves aligned along the X' axis

degradation of etched surfaces. For this purpose surface profilometry traces were made along two specific directions of the (hk̄0) plates namely the [001] axis and the rotated axis x'. At the end of each etching stage surface profiles and corresponding distributions of slopes were extracted from the digitalized surface traces.

Note that distributions of slopes correspond to surface profiles as measured by the stylus instrument and not to profiles as obtained after determination of a straight mean reference line by splitting and filtering. For convenience we present only results (Figs. 4 to 5) related to two plates which exhibit different behaviours: the (011) plate and the ($\bar{7}30$) plate. Effectively, plates with an angle of cut φ_o in the range

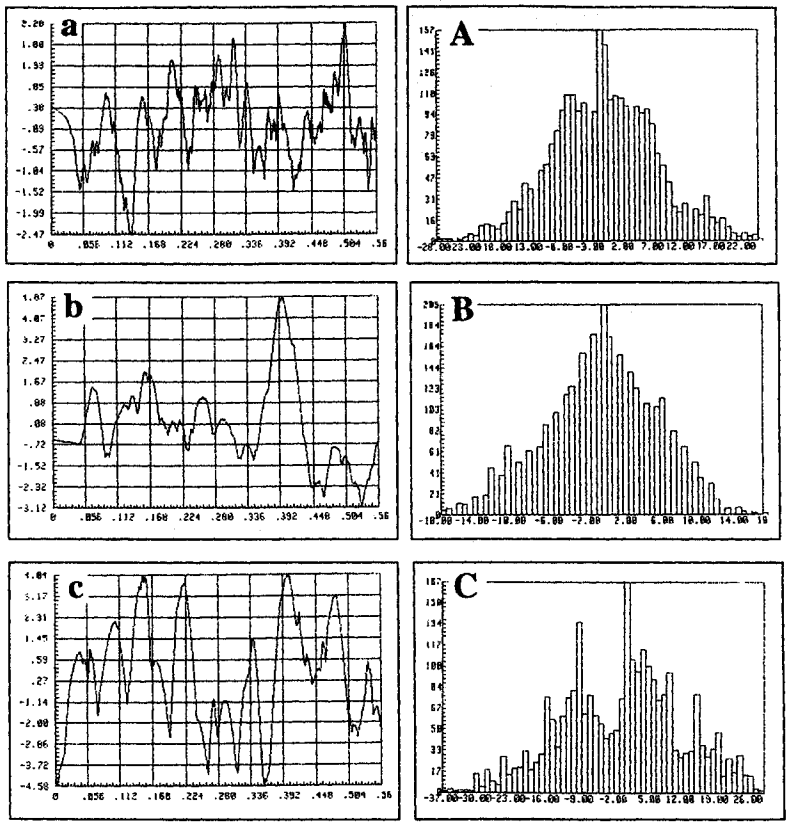

FIGURE 4 X' profilometry traces made on the ($\bar{7}30$) plate after 15 min (a), 30 min (b) and 45 min (c) isothermal etching; A, B, C are the corresponding slope distributions.

[10°, 37°] behave as the ($\bar{7}30$) plate. Moreover the progressive degradation of plates very close from (001) or {011} surfaces ressemble crudely to that observed for {011} plates. As examples, Figures 4 and 5 illustrate, for the two ($\bar{7}30$) and (011) plates the evolution of the X' profilometry traces with the total duration etching t. Because etching causes rapidly the formation of dissolution figures (Fig. 3) which possess stable geometrical features slope distributions do not markedly change with t. But if we turn attention on vertical (R_{max}) and horizontal (L_H) descriptors of profilometry traces we observe a continuous evolution of the lateral extent L_H (Figs. 4 and 5) and for some plates (Fig. 4) a slight increase in R_{max} with prolonged etching.

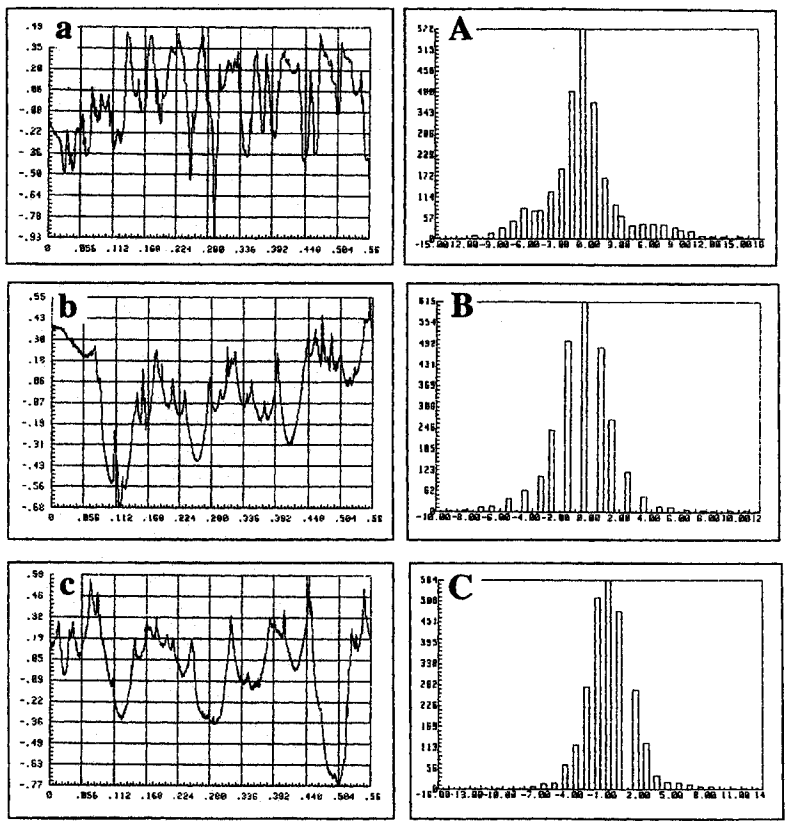

FIGURE 5 X' profilometry traces made on the (011) plate after 15 min (a), 30 min (b) and 45 min (c) isothermal etching; A, B, C are the corresponding slope distributions.

Readers are also invited to examine Tables IV and V which give for various cuts complementary results on R_{max} as well as on the angular range of slope distributions. Because Figure 2 reveals that the dissolution process is only governed by the orientation, φ_o, of plates we can now concentrate our study on final X' and [001] profilometry traces collected in Figure 6.

We observe that the general shape of X' traces changes progressively from concave ([010] plate) alternate concave–convex, convex ([$\bar{2}$10] plate), alternate convex–concave and finally concave ([$\bar{1}$10] plate) when the angle of cut, φ_o, varies from 0° to 45°. In contrast, for [001] traces, two fundamental etching shapes are depicted in Figures

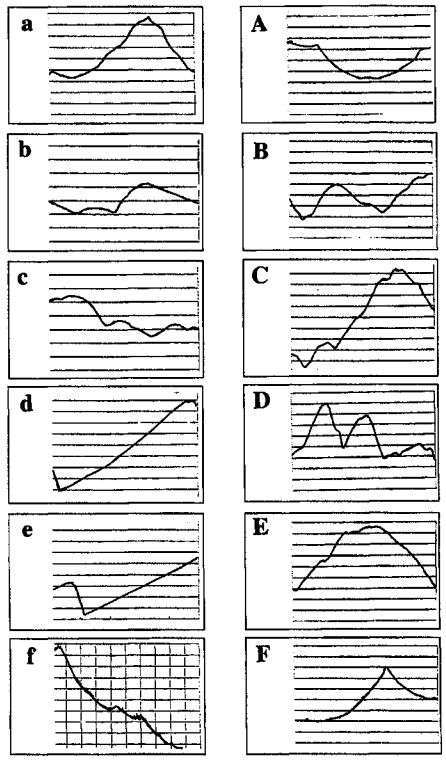

FIGURE 6 X' final profilometry traces for successives plates (a) $\varphi = 0°$, (b) $\varphi = 10°$, (c) $\varphi = 26°$, (d) $\varphi = 34°$, (e) $\varphi = 37°$ and (f) $\varphi = 45°$. A to F are the corresponding Z final profilometry traces.

6A to 6F: concave for [010] and [$\bar{1}$10] plates and convex for φ_o ranging from 10° to 37°.

Moreover numerical treatment of traces (Fig. 7) allows us to follow changes in the root-mean square roughness *Rq* and in the horizontal descriptior L_H with orientation. As these two parameters are of prime importance for micromachining applications complementary plots which illustrate the influence of the angle of cut φ_o are displayed in Figure 7.

Figure 7a indicates that the degradation of etched surfaces is more marked for ($\bar{h}$k0) plates lying between ($\bar{4}$10) and ($\bar{4}$30) plates with an r.m.s. roughness *Rq* which reaches 1,2 μm or more for the two traces made along X' and [001] axes. It should be also noticed that for these

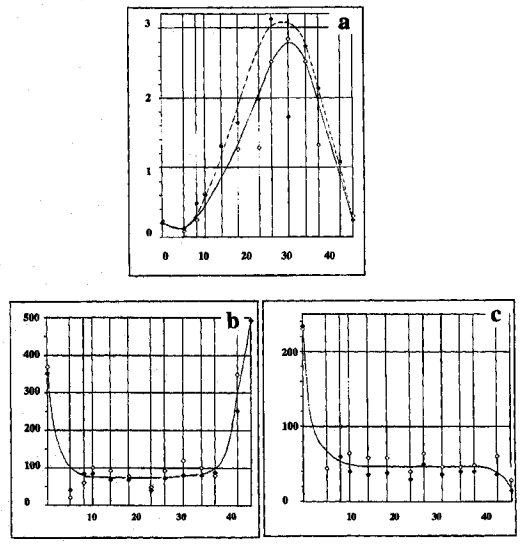

FIGURE 7 (a) Evolution of the root-mean-square roughness parameter Rq with φ_o along X' axis ◇ and along ⟨100⟩ axis ◆. Variation of the horizontal descriptor L_H with φ_o along respectively X' (b) and (010) axis (c).

orientations the parameter R_{max} can take values higher than 10 μm after 45 min etching. Moreover examination of Figures 7b and 7c reveals that for φ_o in the range [10°, 37°] the horizontal description L_H remains unsensitive to orientation for the two traces investigated here. In fact only [010] and [$\bar{1}$10] plates depart from this behaviour with a very large lateral extent in the X' direction and with subsequent a very moderate surface degradation characterized by $Rq < 0{,}5$ μm (Fig. 7a).

2.4. Etched Cross-sectional Sections

First it is of interest to undertake a study of changes in the shape of out-of-roundness profiles with the total duration of etching in order to show how cross-sectional shapes are altered by prolonged etching. For this purpose successive diagrams as obtained after the three etching stages are shown in Figure 8 for two different cross-sections. After a critical etching time, t_c, of about 30 min out-of-roundness profiles of Figures 8c and 8C exhibit a characteristic shape with in particular the formation of peaks and valleys whose angular positions seem

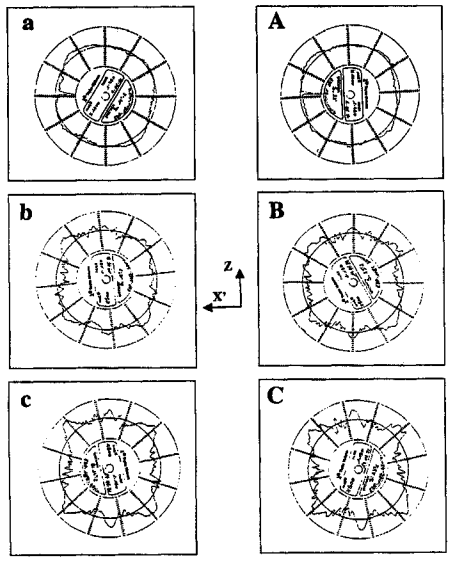

FIGURE 8 Evolution of out-of-roundness profiles related to $(\bar{7}30)$ (a, b, c) and (110) (A, B, C) for $\Delta t = 15$ min, $\Delta t = 30$ min and $\Delta t = 45$ min.

to remain unaffected by prolonged etching showing here again the stability of the etching process. We note also that very rough dissolution figures are produced on the contour of plates so that secondary peaks appear on the final diagrams (Figs. 8c and 8C) which can mask the possible presence of secondary maxima or minima on the final out-of-roundness profiles. Nevertheless approximate final shapes (Fig. 9) can be proposed for the out-of-roundness profiles related to various etched $(\bar{h}k0)$ cross-sections. Examination of these final profiles reveals several interesting features.

(i) The four-fold symmetry about the [010] axis and the combined two-fold and mirror symmetries associated with {100} axes are verified by (010) and $(\bar{h}k0)$ etched plates respectively, as expected for class m3m. Thus the etching process is essentially determined by orientation.

(ii) The most important changes in the general shape of etched cross-sections are observed for φ_o ranging from 0° to 18° with in particular the progressive modification in the peak M_1 centered on the X' axis. Moreover for $23° \leq \varphi_o \leq 45°$ all final profiles (Figs. 8c

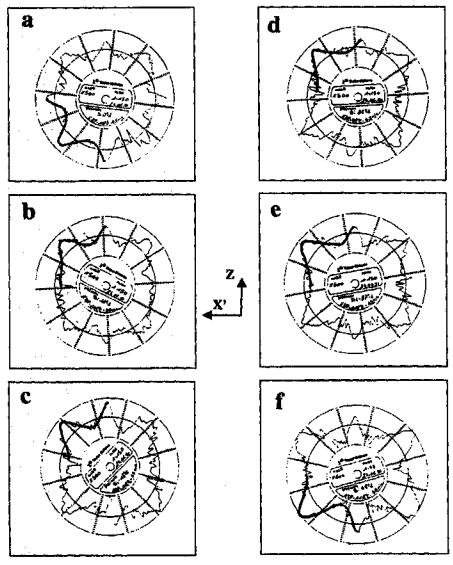

FIGURE 9 Orientation effect in the final out-of-roundness profiles related to various (hk0) sections. (a) to (f) are for $\varphi_o = 0$, $\varphi = 10°$, $\varphi = 18°$, $\varphi = 26°$, $\varphi = 37°$ and $\varphi = 45°$.

and 9c to 9f) exhibit general shapes which at the first sight seem close together.

(iii) Owing to the stability of the dissolution process we can study effects of the angle of cut on the angular positions, Ψ_M and Ψ_m, of major peaks and valleys detected on the various profiles of Figure 9. For φ_o in the range [26°, 45°] all out-of-roundness profiles are characterized by the progessive increase in the maximum M_2 (Figs. 9c to 9f). The angular position of this maximum as measured (Figs. 9d to 9f) with respect the X' axis is found to be $\Psi_{M2} \cong 36°$. Thus in fact this peak is associated with the dissolution slowness $\vec{L}$ {111} [2] related to {111} planes which etch very slowly.

3. DISCUSSION

At this point it seems interesting to compare behaviours for EDP, KOH 35% [2, 5] and TMAH 25% in weight [7] with a special attention on results which are of practical interest for wet micromachining. First

of all let us consider the etch rates of various {hk0} planes for the three etching baths. In practice the temperature of etching is determined by the nature of the etching bath [6] so it seems more appropriate to undertake comparison for etch rates, $R_{\{hk0\}}/R_{\{100\}}$, normalized with respect to {100} plane. Normalized rates collected in Table III illustrate conveniently changes induced by the angle of cut φ_o. We observe that the overall change in $R_{\{hk0\}}/R_{\{100\}}$ is more marked for EDP etchant than for the two other etching solutions. In contrast with KOH 35% and TMAH 25% {100} and {110} planes exhibit quite similar etch rates for EDP. For the three etchants the maximun etch rate occurs for plates close to {120} plane and it is more accentuated for EDP. This behavior is in close agreement with that reported in litterature, [2, 5–7] in particular discrepancies less than 10% are observed for the normalized $R_{\{110\}}/R_{\{100\}}$ etch rate in KOH [2] and TMAH [6, 7]. Thus Table III reveals that the anisotropy of the chemical attack by EDP differs from that characterizing the other etching solutions.

Now emphasis must be placed on the degradation of etched surfaces. Previously published SEM images on surfaces etched in KOH 35% [2, 9] and TMAH 25% [7, 9] show that in fact the geometrical features of dissolution figures produced by EDP on {hk0} plates ressemble crudely to those formed by TMAH. Differences are observed only for {110} plane with grooves which are flatter and more elongated in EDP than in TMAH. This observation may be correlated to the deviations in corresponding normalized $R_{\{110\}}/R_{\{100\}}$ etch rates (Tab. III). Moreover for φ_o in the range (23°–37°) dissolution figures produced by the KOH 35% solution are more rounded that those formed by EDP. Tables IV and V give more information on the degradation of etched surfaces. Comparison of final slope distribu-

TABLE III Values of normalized etch rates, $R_{\{hk0\}}/R_{\{100\}}$ for the three etchants

	Etchants		
φ_o(°)	*EDP*	*KOH* 35%	*TMAH* 25%
14°	1,85	1,59	1,78
26°	2,74	2,19	2,05
34°	1,72	2,08	1,9
45°	1,08	1,94	1,6

TABLE IV Final distributions of slopes as measured from X' and [001] profilometry traces made on {hk0} surfaces deeply by the three etchants

	EDP		*TMAH* 25%		*KOH* 35%	
φ_o(°)	*X' axis*	[001] *axis*	*X' axis*	[001] *axis*	*X' axis*	[001] *axis*
0	± 2,5°	± 2,5°	± 3°	± 3°	± 2°	± 2°
10	−4°, +6°	± 8°	−5°, +9°	± 3°	± 5°	± 5°
18	−7°, +18°	± 20°	± 1,5°	± 3°	−4°, +6°	± 6°
26	−16°, +13°	± 22°	−9°, +8°	± 16°	± 4°	± 7°
37	−16°, +8°	± 24°	−10°, +5°	± 14°	−9°, +7°	± 10°
45	± 1°	± 1°	± 1.5°	± 1,5°	± 2°	± 14°

TABLE V Values of maximum peak to valley roughness, R_{max}, evaluated on {hk0} surfaces etched 45 min in EDP and KOH

	R_{max} (μm)	
φ_o (°)	*EDP*	*KOH* 35%
0°	8	4
10°	6,1	1,8
14°	18	1,4
23°	21,7	1,5
26°	28,2	3
37°	22,5	4
42°	23	3
45°	0,9	2,4

tions (Tab. IV) reveals that more surfaces are covered by slopy dissolution figures when etched by EDP and that the angular range of slopes is the more reduced for KOH 35% ({110} plane excepted). Values for the maximum peak to valley roughness, R_{max}, as evaluated from profilometry traces made on {hk0} surfaces etched in EDP and KOH which behave differently are collected in Table V. As soon as the orientation of plates deviates from 14° from {100} plane and from 3° from {110} planes the parameter R_{max} can reach values greater than 18 μm for EDP where as values smaller than 4 μm are usually measured for KOH. It must be also outlined that R_{max} is very small ($R_{max} \cong 0{,}9\,\mu m$) for {110} surfaces etched in EDP in contrast with behaviour for KOH.

As geometrical features of etched {hk0} surfaces depend on the orientation of plates it might be of interest to follow theoretically the changes in dissolution figures and surface roughness with the angle of cut φ_o. This may be done using the simulator TENSOSIM [10, 11] based on the tensorial model for the anisotropic dissolution [12–14]

provided the database of the simulator composed of dissolution constants was determined from experiments. It has been previously shown [15, 16] that by analysing changes in 2D etching shapes such as out-of-roundness profiles and profilometry traces it becomes possible to evaluate the dissolution constants. The data-base is sufficiently accurate when we start with X_1 profilometry traces and {hk0} out-of-roundness profiles whose progressive evolutions with φ_o are easily distinguishable. Experimental results of Sections 2.3 and 2.4 reply to this need. Consequently tentative will be made in a future paper to firstly determine the database for EDP and secondly derive theoretical 2D etching shapes.

4. CONCLUSION

Changes in etch rate and in geometrical features of etched {hk0} surfaces are extensively studied and then compared with results related to other etchants (KOH 35%, TMAH 25%). The chemical attack in EDP is highly anisotropic and lead to a marked degradation of etched surfaces for φ_o in the range [10°–42°].

However {110} plates are rather polished by EDP and the roughness of {100} plates is quite the same for EDP, KOH and TMAH. So these two orientations are interesting for micromachining applications. Changes in the shape of out-of-roundness profiles with the angle of cut reveal the influence of {111} plane for φ_o in the range (26° – 45°) and a progressive evolution of shapes which can be conveniently used to evaluate the dissolution constants characterizing the anisotropy of the EDP etchant.

References

[1] Petersen, K. E. (1982). "Silicon as a mechanical material", *Proc. IEEE*, **70**, 420–457.
[2] Tellier, C. R. and Brahim-Bounab, A. (1994). "Anisotropic etching of silicon crystals in KOH solution Part I: Experimental etched shapes and determination of the dissolution slowness surface", *J. Mat. Sci.*, **29**, 5953–5971.
[3] Sato, K., Shikida, M., Yamashiro, T., Tsunekawa, M. and Ito, S. (1999). "Roughening of single-crystal silicon surface etched by KOH water solution", *Sensors and Actuators*, **73**, 122–130.
[4] Seidel, H., Csepregi, L., Neuberger, A. and Baumgartel, H. (1990). "Anisotropic etching of crystalline silicon in alkaline solutions", *J. Electrochem. Soc.*, **137**, 3612–3626.

[5] Brahim-Bounab, A., *Thesis 279*, University of Franche-Comté, Besancon, France, 25 September, 1992.
[6] Sato, K., Shikida, M., Yamashiro, T., Asaumi, K. and Iriye, Y. (1999). "Anisotropic etching rates of single-crystal silicon for TMAH water solution as a function of crystallographic orientation", *Sensors and Actuators*, **73**, 131–137.
[7] Charbonnieras, A. R. and Tellier, C. R. (1999). "Characterization of the anisotropic chemical attack of {hk0} silicon plates in a TMAH solution. Determination of a database", *Sensors and Actuators*, **77**, 81–97.
[8] Tellier, C. R. and Durand, S., "Micro-fabricated silicon structures: experimental and theoretical investigation of 3D etched shapes", *9th EFTF* Besançon, France, 8–10 March, 1995, pp. 426–429.
[9] Tellier, C. R., Charbonnieras, A. and Leblois, T. (1990). "A comparative study for the chemical etching of {hk0} silicon plates in EDP, KOH and TMAH solution", *Advances in Sciences and Technology 26, Solid State Chemical and Biochemical Sensors*, Vincenzini, P. et Dori, L. Eds.), pp. 527–534.
[10] Tellier, C. R. and Durand, S. (1997). "Micromachining of (hhl) silicon structures: Experiments and 3D simulation of etched shapes", *Sensors and Actuators*, **460**, 168–175.
[11] Tellier, C. R. (1998). "Anisotropic etching of silicon crystals in KOH solution. Part II: experimental and theoretical shapes for 3D structures micro-machined in (hk0) platers", *J. Mat. Sci.*, **33**, 117–131.
[12] Tellier, C. R. and Vaterkowski, J. L. (1989). "A tensorial representation of the dissolution slowness . Applications to etched singly rotated quartz plates", *J. Mater. Sci.*, **24**, 1077–1088.
[13] Tellier, C. R. (1989). "A three-dimensional kinematic model for the dissolution of crystals", *J. Cryst. Growth*, **96**, 450–452.
[14] Brahim-Bounab, A. and Amaudrut, J. Y. and Tellier, C. R., "*Dissolution slowness surfaces of cubic crystals. Part 1: Theory and three-dimensional representation for class 23*".
[15] Tellier, C. R. and Brahim-Bounab, A. (1994). "Anisotropic etching of silicon crystals in KOH solution. Part II: Theoretical two- dimensional etched shapes discussion of the adequation of the dissolution slowness surface", *J. Mat. Sci.*, **29**, 6354–6378.
[16] Leblois, T. and Tellier, C. R., "Determination of the dissolution slowness surface by study of etched shapes. *J. Morphology of the dissolution slowness surface and theoretical etched shapes*", *J. Phys. III France*, **2**.